J Ginseng Res 45 (2021) 295–304

Contents lists available at ScienceDirect

Journal of Ginseng Research

journal homepage: http://www.ginsengres.org

Research Article

20(*S*)-ginsenoside Rh2 induces caspase-dependent promyelocytic leukemia-retinoic acid receptor A degradation in NB4 cells via Akt/Bax/caspase9 and TNF-α/caspase8 signaling cascades

Sirui Zhu [1,☆], Xiaoli Liu [1,☆], Mei Xue [2], Yu Li [1], Danhong Cai [1], Shijun Wang [3], Liang Zhang [1,*]

[1] *Jiangsu Key Laboratory for Pharmacology and Safety Evaluation of Chinese Materia Medica, School of Pharmacy, Nanjing University of Chinese Medicine, Nanjing, Jiangsu, 210023, PR China*
[2] *College of Basic Medical Sciences, Institute of TCM-related Comorbid Depression, Nanjing University of Chinese Medicine, Nanjing, Jiangsu, 210023, PR China*
[3] *Shandong co-innovation center of TCM formula, College of Traditional Chinese Medicine, Shandong University of Traditional Chinese Medicine, Jinan, Shandong, 250035, PR China*

ARTICLE INFO

Article history:
Received 29 September 2019
Received in Revised form
20 March 2020
Accepted 7 May 2020
Available online 15 May 2020

Keywords:
Acute promyelocytic leukemia
Apoptosis
Caspase
20(*S*)-ginsenoside Rh2
PML-RARA

ABSTRACT

Background: Acute promyelocytic leukemia (APL) is a hematopoietic malignancy driven by promyelocytic leukemia–retinoic acid receptor A (PML-RARA) fusion gene. The therapeutic drugs currently used to treat APL have adverse effects. 20(*S*)-ginsenoside Rh2 (GRh2) is an anticancer medicine with high effectiveness and low toxicity. However, the underlying anticancer mechanisms of GRh2-induced PML-RARA degradation and apoptosis in human APL cell line (NB4 cells) remain unclear.

Methods: Apoptosis-related indicators and PML-RARA expression were determined to investigate the effect of GRh2 on NB4 cells. Z-VAD-FMK, LY294002, and C 87, as inhibitors of caspase, and the phosphatidylinositol 3-kinase (PI3K) and tumor necrosis factor-α (TNF-α) pathways were used to clarify the relationship between GRh2-induced apoptosis and PML-RARA degradation.

Results: GRh2 dose- and time-dependently decreased NB4 cell viability. GRh2-induced apoptosis, cell cycle arrest, and caspase3, caspase8, and caspase9 activation in NB4 cells after a 12-hour treatment. GRh2-induced apoptosis in NB4 cells was accompanied by massive production of reactive oxygen species, mitochondrial damage and upregulated Bax/Bcl-2 expression. GRh2 also induced PML/PML-RARA degradation, PML nuclear bodies formation, and activation of the downstream p53 pathway in NB4 cells. Z-VAD-FMK inhibited caspase activation and significantly reversed GRh2-induced apoptosis and PML-RARA degradation. GRh2 also upregulated TNF-α expression and inhibited Akt phosphorylation. LY294002, an inhibitor of the PI3K pathway, enhanced the antitumor effects of GRh2, and C 87, an inhibitor of the TNF-α pathway, reversed NB4 cell viability, and GRh2-mediated apoptosis in a caspase-8-dependent manner.

Conclusion: GRh2 induced caspase-dependent PML-RARA degradation and apoptosis in NB4 cells via the Akt/Bax/caspase9 and TNF-α/caspase8 pathways.

1. Introduction

Acute promyelocytic leukemia (APL), also known as acute myeloid leukemia M_3(AML M_3), is characterized by chromosome t(15;17) (q22;q12) translocation, leading to formation of the PML-RARA fusion protein [1,2]. PML, a proapoptotic protein, and RARA, a hematopoietic differentiation protein, are blocked via dominant negative inhibition [3]. Furthermore, many naive leukemia cells in the bone marrow and other hematopoietic tissues that have lost differentiation and apoptosis functions unrestrictedly proliferate and enter the peripheral blood, whereas normal blood cell production is markedly inhibited [4]. Encouraging progress has been

* Corresponding author. Jiangsu Key Laboratory for Pharmacology and Safety Evaluation of Chinese Materia Medica, School of Pharmacy, Nanjing University of Chinese Medicine, Nanjing, Jiangsu, 210023, PR China.
E-mail address: Zhangl_1999@163.com (L. Zhang).
☆ These authors have contributed equally to this work.

https://doi.org/10.1016/j.jgr.2020.05.001
p1226-8453 e2093-4947/$ – see front matter

made in APL treatment with the use of retinoic acid (ATRA) and arsenic trioxide (ATO). ATO mainly affects the PML portion of the PML-RARA fusion protein and induces apoptosis in APL cells. ATRA mainly acts on the RARA portion of the fusion protein and induces APL cell differentiation. Both can promote degradation of the PML-RARA fusion protein [2,5]. PML-RARA is degraded via three mechanisms: proteasome degradation, which is also the main mechanism in ATO-induced fusion protein degradation [3,6], autophagy-dependent degradation [7], and caspase-dependent degradation [8,9]. The latter two are partially involved in ATRA-induced fusion protein degradation [10]. However, the widespread use of ATO and ATRA causes some adverse reactions including systemic infections, coagulation, fibrinolysis disorders, hyperleukocytosis, and secondary leukemia. In addition, some patients do not respond to PML-RARA–targeted therapy or relapse after complete remission [11–13]. Therefore, a minimally toxic and highly targeted treatment for APL is urgently needed.

20(*S*)-Ginsenoside Rh2 (GRh2) is the major anticancer ingredient in ginseng, which has high efficiency and low toxicity, and is widely used to treat gastric cancer, liver cancer, breast cancer, and leukemia [14–17]. Its main anticancer mechanisms include apoptosis promotion, cell cycle inhibition, and cancer cell differentiation [17–20]. Many reports have clarified that caspase family proteins are the key targets of GRh2 [18,20,21]. GRh2 promotes caspase8, caspase9, and caspase3 activation in various cancer cells, thus inducing caspase-dependent apoptosis in cancer cells via multiple pathways [18,20,21]. However, the effect of GRh2 on human acute promyelocytic leukemia cells (NB4 cells) remains unreported. As described above, the caspase pathway is involved in degrading the PML-RARA protein. Therefore, whether GRh2 can degrade the PML-RARA fusion protein in NB4 cells in a caspase-dependent manner requires investigation.

The PI3K/Akt signaling pathway plays an essential role in regulating apoptosis and cell cycle progression, which are widely activated in leukemia [22–24]. GRh2-induced cell cycle arrest and apoptosis via PI3K/Akt signaling pathway inhibition has been widely reported [20,23,25]. Reports have indicated that TNF-α is a crucial target protein for GRh2-induced apoptosis in cancer cells [26]. In addition, PI3K/Akt and TNF-α are closely correlated with caspase9 and caspase8 activation [26,27]. Therefore, we investigated whether upstream PI3K/Akt and TNF-α signaling pathways in NB4 cells regulate GRh2-induced caspase-dependent apoptosis and PML-RARA degradation.

In the present study, we aimed to determine whether GRh2 promotes PML-RARA protein degradation in NB4 cells in a caspase-dependent manner, and whether this process is achieved via the PI3K/Akt and TNF-α signaling pathways. Our results provide a foundation for developing GRh2 for APL adjuvant therapy. Fusion protein degradation through the caspase pathway is independent of the ATRA resistance mechanism, which provides new insight for treating ATRA-resistant APL.

2. Materials and methods

2.1. Materials

20(*S*)-ginsenoside Rh2 (98.0% purity) and ATRA(99.74% purity) were obtained from MedChemExpress (Monmouth Junction, NJ, USA). Z-VAD-FMK and cycloheximide (CHX) were obtained from ApexBio (Houston, TX, USA). N-acetyl-L-cysteine (NAC), LY294002, and C 87 were purchased from MedChemExpress. PML-RARA antibody was purchased from Abcam (Cambridge, MA, USA). Cleaved-caspase3 and cleaved-PARP antibodies were obtained from Cell Signaling Technology (Danvers, MA, USA). glyceraldehyde-3-phosphate dehydrogenase (GAPDH), Bax, Bcl-2, pro-caspase3, TNF-α, and PML antibodies were purchased from Proteintech (Chicago, IL, USA). t-Akt, p-Akt, Fas, and TNFR1 antibodies were obtained from Affinity Biosciences (Cincinnati, OH, USA).

2.2. Cell cultures

NB4 cells were purchased from BeNa Culture Collection (Beijing, China). The cells were cultured in RMPI 1640 medium (Gibco, Grand Island, NY, USA) containing 10% fetal calf serum (Gibco) at 37°C and 5% CO_2.

2.3. Cell viability assays

A cell counting kit-8 (CCK-8) kit for detecting cell viability was purchased from Beyotime Biotechnology Co., Ltd. (Nanjing, Jiangsu, China). Briefly, cells were seeded at 5×10^4 cells/mL in a 96-well plate at 200 μL per well. Then, 20 μL of CCK-8 was added per well after applying different concentrations of the GRh2 for 12 hours. Cells were incubated for 2 h in a 37°C incubator. The absorbance was measured at 450 nm using a microplate reader (TECAN, Männedorf, Switzerland).

2.4. Transmission electron microscopy

Cell samples were collected, then fixed in 2.5% glutaraldehyde for 24 h and in 1% citric acid for 2 h. The cells were dehydrated through increasing concentrations of alcohol. Acetone and embedding agents were then used to infiltrate the cells, which were incubated overnight at 37°C. The cells were polymerized in a 60°C oven for 48 h, sliced using an ultramicrotome, stained with uranium lead, and observed under a transmission electron microscope after drying overnight (HT7700-Hitachi, Tokyo, Japan).

2.5. Hoechst33258 staining

An Apoptosis-Hoechst staining kit was used to detect apoptosis (Beyotime Biotechnology Co., Ltd.,). After the cells were collected, fixed, washed twice with phosphate-buffered saline (PBS), stained with Hoechst 33258 staining solution for 5 min, washed again with PBS, and observed under a fluorescence microscope (Nikon, Tokyo, Japan). The excitation light wavelength was 350 nm, and the emission light wavelength was 460 nm.

2.6. Flow cytometry for apoptosis

Annexin V-Alexa Fluor-647/propidium iodide (PI) double staining was used to detect apoptosis (Fcmacs Biotechnology, Nanjing, Jiangsu, China). NB4 cells were seeded at 1×10^5 cells/mL in six-well plates containing different concentrations of drug medium, incubated for 12 hours, and harvested. Next, 100 μL of binding buffer was added to adjust the cell density to 1×10^6 cells/mL, then 5 μL of AnnexinV/Alexa Fluor 647 and 10 μL of 20 μg/mL PI were added to each sample and incubated in the dark for 15 min. Apoptosis was detected via flow cytometry (Biosciences Accuri C6; BD Biosciences, Franklin Lake, NJ, USA).

2.7. Western blot

NB4 cells were seeded at 1×10^5 cells/mL in cell culture dishes containing different concentrations of drug medium, then harvested after 12 hours of incubation. Total protein was extracted by lysing the lysate (RIPA: PMSF: protein phosphatase inhibitor = 100:1:1), and the protein concentration was determined using the Bradford method. The extracted protein was separated and transferred to a nitrocellulose membrane (Millipore,

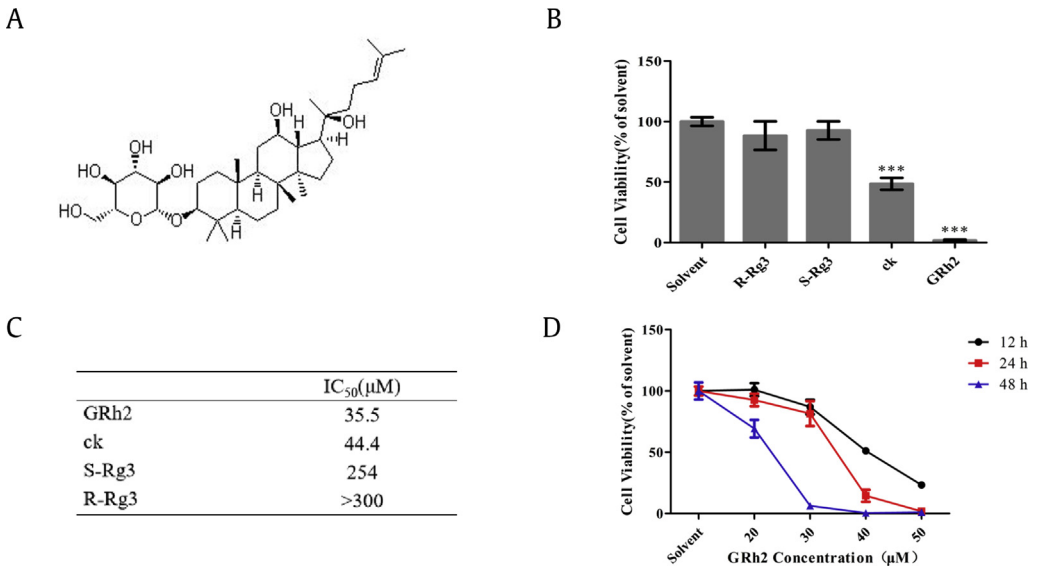

	IC_{50}(μM)
GRh2	35.5
ck	44.4
S-Rg3	254
R-Rg3	>300

Fig. 1. GRh2 inhibited NB4 cell viability. (A) GRh2 chemical structure. (B) NB4 cells were incubated with 50 μM rare diol-type ginsenoside R-Rg3, S-Rg3, ck, GRh2 for 24 h, and cell viability was determined via CCK-8 assay. The result are shown as the mean ± SD (n = 6) ***$p < 0.001$ versus solvent. (C) IC_{50} values of GRh2, ck, S-Rg3, and R-Rg3 in NB4 cells (24 h). (D) Different concentrations of GRh2 were incubated with NB4 cells for 12, 24, and 48 h, and cell viability was determined via CCK-8 assay. The results are shown as the mean ± SD (n = 6).
GRh2, 20(*S*)-*ginsenoside Rh2.*

Billerica, MA, USA) using 8−12% SDS-PAGE separation gel, then blocked with TBST containing 5% skim milk powder. The primary antibody was incubated overnight at 4°C, and then the secondary antibody was incubated for 1 h and scanned using a gel imager (Bio-Rad, Hercules, CA, USA).

2.8. Immunofluorescence

NB4 cells were seeded at 1×10^5 cells/mL in cell culture dishes containing drug medium, then harvested after 8 hours of incubation, washed with PBS, fixed with 4% paraformaldehyde for 30 min, and then permeabilized with 0.1% Triton X-100 for 10 min. The cells were blocked with 5% bovine serum albumin for 30 min, then incubated with 5% bovine serum albumin:PML antibody (280 μg/mL) = 1:100. Cells were washed the next day and incubated with the secondary antibody. The nuclei were stained with 4',6-diamidino-2-phenylindole (DAPI) and observed under a fluorescence microscope (Nikon).

2.9. JC-1 staining

A mitochondrial membrane potential detection kit (JC-1) was used to detect the mitochondrial membrane potential detection (Beyotime Biotechnology Co. Ltd.) per the manufacturer's instructions. Briefly, the cells were collected, and then JC-1 staining working solution was added. Cells were incubated at 37°C for 20 min. After the incubation, the cells were washed twice in JC-1 staining buffer, and the red and green fluorescence was observed under a fluorescence microscope (Nikon).

2.10. Caspase8 and caspase9 enzyme activity detection

Caspase8 and caspase9 enzyme activity assay kits (Beyotime Biotechnology Co. Ltd.) were used to detect caspase8 and caspase9 enzyme activity. The cells were lysed in an ice bath for 30 min and centrifuged at 16000 g for 15 min. The protein was collected, and the protein concentration was determined using the Bradford method. Ac-IETD-pNA and Ac-LEHD-pNA were applied at 37°C for 12 h. Finally, the absorbance at A_{405} was detected using a microplate reader (TECAN).

2.11. DNA content determination

A cell cycle assay kit was used to determine the cellular DNA content per the manufacturer's instructions(Fcmacs Biotech Co. Ltd.).Briefly, the cells were collected and washed in 75% ethanol for 12 h, then 400 μL of staining buffer, 15 μL of PI staining solution, and 4 μL of RNase A (2.5 mg/mL) were added per 1×10^6 cells, incubated at 37°C for 30 minutes in the dark, and immediately detected via flow cytometry (Accuri C6; BD Biosciences).

2.12. Reactive oxygen species detection

A Reactive Oxygen Species Detection Kit (Beyotime Biotechnology Co. Ltd.) was used to detect intracellular reactive oxygen species per the manufacturer's instructions. Cells (1×10^6) were suspended in 1 mL of 10 μM 2',7'-Dichlorodihydrofluorescein diacetate (DCFH-DA), incubated at 37°C for 20 min, and washed thoroughly, then the fluorescence was read using a fluorescent microplate reader (TECAN) or fluorescence microscope (Nikon) at an excitation wavelength of 488 nm and an emission wavelength of 525 nm.

2.13. Real-time PCR

NB4 cells (2×10^6) were collected per sample, and total RNA was extracted using TRIzol reagent (Invitrogen, Carlsbad, CA, USA) per the manufacturer's instructions. The cDNA was reverse transcribed into cDNA using the 5X All-In-One RT MasterMix Reverse Transcription Kit (Abm, New York City, NY, USA). The EvaGreen 2X qPCR MasterMix reagent (Abm) was used, with a 10 μL PCR reaction volume. Primers were supplied by Abm Bio. The relative expression level of the target gene was calculated using the $2^{-\triangle\triangle CT}$ method,

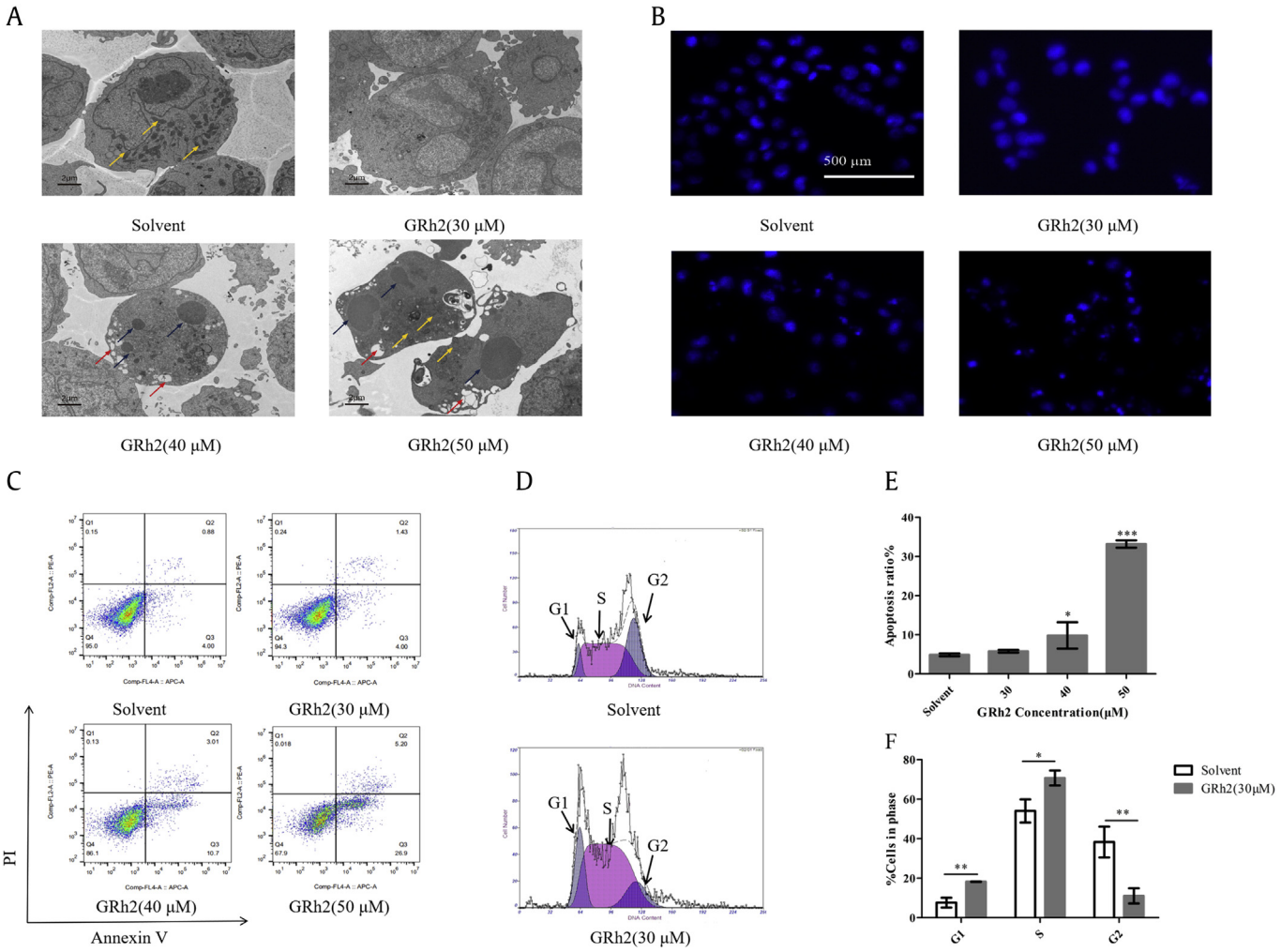

Fig. 2. GRh2 induced G1/S cycle arrest and apoptosis in NB4 cells. NB4 cells were incubated with 30 μM, 40 μM, or 50 μM GRh2 for 12 h. (A) NB4 intracellular microstructure was observed via transmission electron microscopy. (B) Hoechst33258 staining was used to observe changes in nuclear morphology of NB4 cells after GRh2 administration Scale bar=500 μm. (C) Representative image of the change in apoptotic proportion in NB4 cells after drug application, Annexin V/PI double staining assay was used. (D) NB4 cells were incubated with 30 μM GRh2 for 12 h, and representative images of NB4 cell cycle distribution after PI staining are shown. (E) Quantitative statistical graph of changes in the apoptotic proportion. The results are shown as the mean ± SD (n = 3) $*p < 0.05$, $***p < 0.001$ versus solvent. (F) Quantitative statistical graph of cell cycle distribution. The result are shown as the mean ± SD (n = 3) $*p < 0.05$, $**p < 0.01$.
GRh2, 20(*S*)-*ginsenoside Rh2*.

and GAPDH was used as the endogenous control. Real-time PCR primers for the target genes were as follows:

PML-RARA [L type [28], According to accession numbers M73778 (*PML*) and X06538 (*RARA*)] [28]
Primer F 5′TCTTCCTGCCCAACAGCAA3′
Primer R 5′GCTTGTAGATGCGGGGTAGAG3′
TNF-α (NM_000594)
Primer F 5′AGGGACCTCTCTCTAATCAGC3′
Primer R 5′AGGACCTGGAGTAGATGAG3′
TP53 (NM_000546)
Primer F 5′CTCCTCAGCATCTTATCCG3′
Primer R 5′GGCACCACCACACTATGTC3′
GAPDH (NM_002046)
Primer F 5′CACCATCTTCCAGGAGCGAG3′
Primer R 5′AAATGAGCCCCAGCCTTCTC3′

2.14. Statistical analysis

Statistical analysis was performed using GraphPad Prism5 software (GraphPad Software Inc. CA, USA), and all data are expressed as the mean ± SD. A *t* test was used for comparisons between two groups, and one-way analysis of variance was used for comparison between multiple groups. A value $p < 0.05$ was considered statistically significant.

3. Results

3.1. GRh2 inhibited cell viability in NB4 cells

Rare diol-type ginsenosides have protopanaxadiol as as the parent nucleus and differ in their conformations and glycosyl numbers. Among them 20(*S*/*R*)-ginsenoside Rg3(S/R-Rg3), GRh2, and compound K (ck) are the most effective anticancer components in ginseng [23,29,30]. NB4 cells were incubated with 50 μM R-Rg3, S-Rg3, ck, and GRh2 for 24 h. GRh2 and ck significantly inhibited NB4 cell viability, and GRh2 showed the strongest inhibitory effect (Fig. 1B). Fig. 1A shows the GRh2 structure. NB4 cells were incubated with different concentrations of R-Rg3, S-Rg3, ck, or GRh2 for 24 h, and the resulting IC_{50} values were >300 μM, 254 μM, 44.4 μM, and 35.5 μM, respectively (Fig. 1C). Thus, GRh2 was selected for the

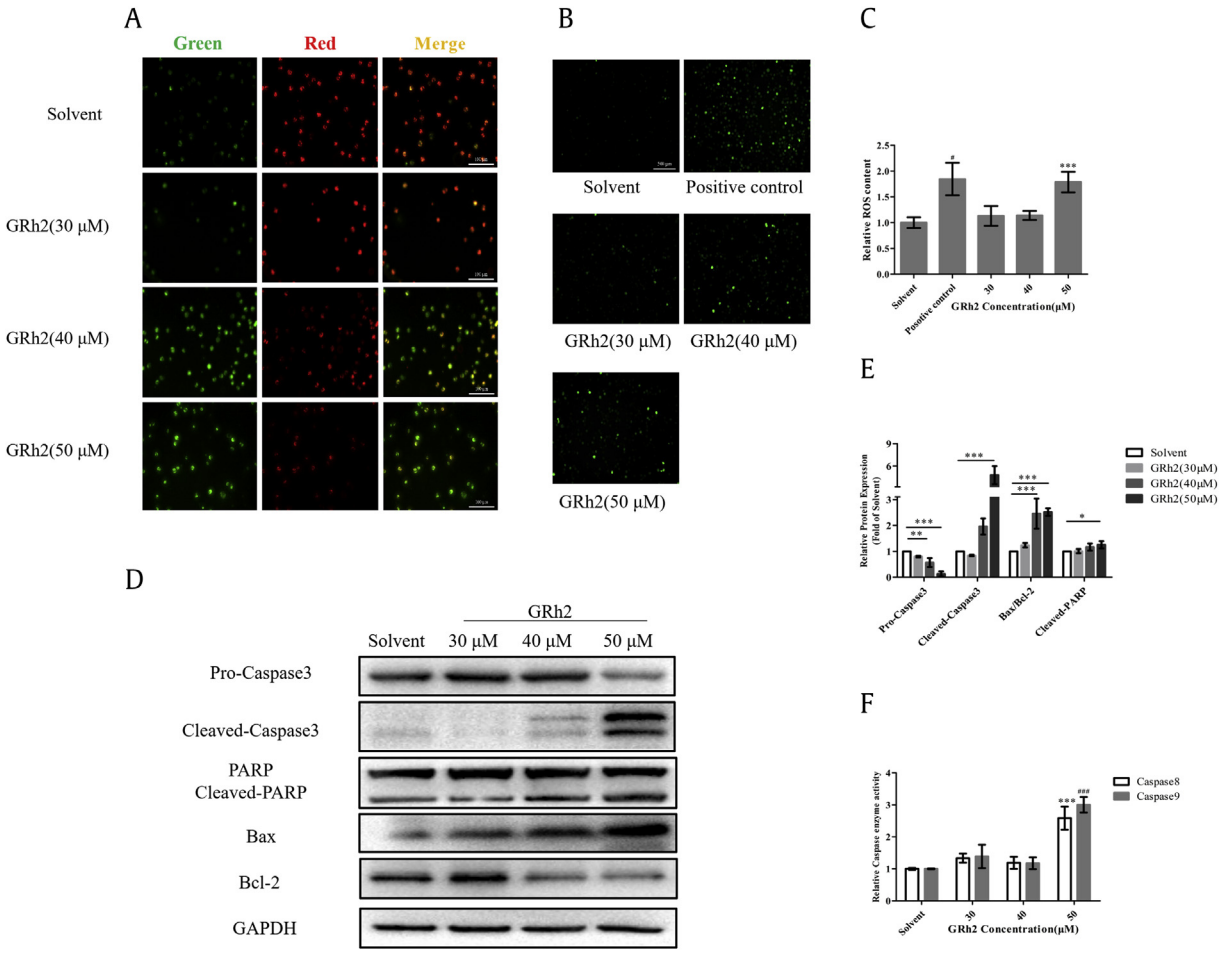

Fig. 3. GRh2 induced mitochondrial damage and caspase activation in NB4 cells. NB4 cells were incubated with 30 μM, 40 μM, and 50 μM GRh2 for 12 h. (A) JC-1 staining was used to observe changes in mitochondrial membrane potential of NB4 cells after administering GRh2 Scale bar=100 μm. Red fluorescence indicates a higher membrane potential, and green fluorescence represents a membrane potential dissipation. (B) The intracellular ROS level of NB4 cells after administering GRh2 was detected via fluorescent-probe DCFH-DA, and a representative picture of three replicates is shown Scale bar=500 μm. (C) Quantitative statistical graph of relative fluorescence intensity of intracellular DCF. The result are shown as the mean ± SD (n = 3) #$p < 0.05$, ***$p < 0.001$ versus solvent. (D) Protein expression levels of pro-caspase3, cleaved-caspase3, Bax, Bcl-2, and cleaved-PARP in NB4 cells were detected via Western Blot. A representative picture of three replicates is shown. (E) Quantitative statistical graph of the relative expression levels of proteins. The results are shown as the mean ± SD (n = 3) *$p < 0.05$, **$p < 0.01$, ***$p < 0.001$. (F) Quantitative statistical graph of caspase8 and caspase9 cleavage activation levels in NB4 cells after administering of GRh2, Ac-IETD-pNA, and Ac-LEHD-pNA methods were used. The results are shown as the mean ± SD (n = 3) ***$p < 0.001$ versus solvent (caspase8), ###$p < 0.001$ versus solvent (caspase9).
GRh2, 20(*S*)-*ginsenoside Rh2; ROS, reactive oxygen species.*

following study. After incubation with different concentrations of GRh2 for 12, 24, and 48 h, the NB4 cell viability decreased dose-dependently (Fig. 1D). GRh2 also showed selectivity between NB4 cells and normal blood cells [23](Fig. S1).

3.2. GRh2 induced G1/S cycle arrest and apoptosis in NB4 cells

As per the above experimental results, 30 μM, 40 μM, and 50 μM GRh2 were incubated with NB4 cells for 12 h. Transmission electron microscopy showed that 40 μM and 50 μM GRh2 induced NB4 cell apoptosis, which was characterized by cytoplasmic vacuolation(red arrows), nuclear condensation and lysis(blue arrows), and mitochondrial ridge disappearance(yellow allows) (Fig. 2A). Hoechst 33258 staining also indicated that the NB4 nuclei shrank and shattered under the action of 40 μM and 50 μM GRh2 (Fig. 2B). AnnexinV/PI double staining showed that 40 μM and 50 μM GRh2 significantly increased the proportion of NB4 apoptotic cells (Fig. 2C, E). GRh2 at 30 μM decreased the NB4 cell viability, and the apoptotic proportion did not significantly differ; thus, we determined the DNA content, and 30 μM GRh2 significantly induced NB4 cell cycle arrest in the G1/S phase (Fig. 2D, F).

3.3. GRh2 induced mitochondrial damage and caspase activation in NB4 cells

We further investigated whether GRh2-induced apoptosis in NB4 cells is accompanied by mitochondrial damage and caspase activation. The JC-1 staining results showed that green fluorescence was significantly enhanced, and mitochondrial membrane potential was significantly decreased after applying different concentrations of GRh2 (Fig. 3A), and we detected a large amount of reactive oxygen species (ROS) production in the cells (Fig. 3B and C). However, NAC, an ROS inhibitor, could not reversed the GRh2-induced decrease in NB4 cell viability (Fig. S2). Western blot results showed that the Bax/Bcl-2 ratio was significantly upregulated after administering GRh2 (Fig. 3D and E). Thus, GRh2 induces

mitochondrial damage during NB4 cell apoptosis accompanied by decreased mitochondrial membrane potential and a large amount of ROS production. We also detected the cleavage activation of caspase8, caspase9, caspase3, and the downstream substrate, PARP, during GRh2-induced apoptosis of NB4 cells (Fig. 3D–F).

3.4. GRh2 induced PML/PML-RARA degradation, PML nuclear body formation, and downstream p53 signaling pathway activation in NB4 cells

PML-RARA is a key effector molecule that drives malignant proliferation of NB4 cells and is also a specific target for NB4 cells [1–3]. Presence of the fusion protein blocks PML NB formation and the activation of the downstream tumor suppressor gene, *TP53* [3]. We investigated the effects of GRh2 on PML-RARA degradation and its downstream gene, *TP53*, in NB4 cells. Western blot results showed that GRh2 significantly induced downregulation of PML and PML-RARA protein levels in NB4 cells (Fig. 4A and B). However, we observed no changes in *PML-RARA* mRNA levels (Fig. 4C). After blocking protein synthesis using CHX, GRh2 increased the PML-RARA degradation rate (Fig. 4D and E), the PML nuclear bodies (NBs) reappeared, and the *TP53* gene was activated (Fig. 4F and G). In conclusion, we suggest that GRh2 degrades the PML-RARA fusion protein in NB4 cells, and the PML or its cleavage site. GRh2 also induced formation of PML NBs and activated the downstream p53 signaling pathway [10,31].

3.5. GRh2-induced apoptosis and PML-RARA degradation in NB4 cells were caspase-dependent

We demonstrated that GRh2 induced caspase activation and degradation of PML/PML-RARA during NB4 cell apoptosis. Reports indicate that PML-RARA cleavage in PML sites dependents on caspase [10]. Therefore, we next verified whether GRh2-induced apoptosis and PML-RARA degradation in NB4 cells depended on caspase. Z-VAD-FMK, a broad-spectrum caspase inhibitor, significantly reversed the GRh2-induced decrease in NB4 cell viability (Fig. 5A) and apoptosis (Fig. 5B and C). Z-VAD-FMK also significantly reversed GRh2-induced degradation of PML-RARA in NB4

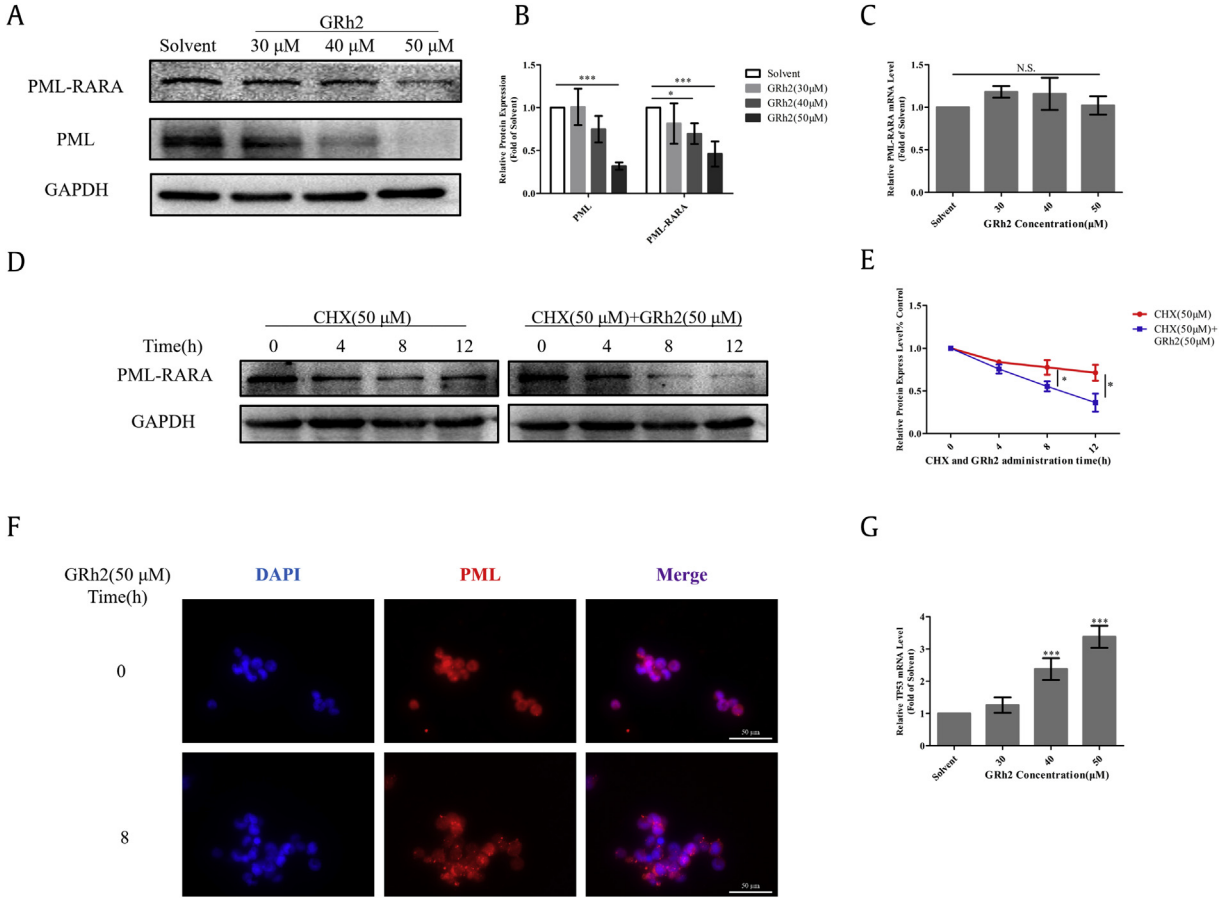

Fig. 4. GRh2 induced PML/PML-RARA degradation, PML NB formation and activation of the downstream p53 signaling pathway in NB4 cells. NB4 cells were incubated with 30 μM, 40 μM, and 50 μM GRh2 for 12 h. (A) Western blot was used to detect PML/PML-RARA expression in NB4 cells after GRh2 administration. A representative picture of three replicates is shown. (B) Quantitative statistical graph of the relative expression levels of proteins. The results are shown as the mean ± SD (n = 3) $^{*}p < 0.05$, $^{***}p < 0.001$. (C) RT-PCR was used to detect the *PML-RARA* mRNA expression level in NB4 cells after GRh2 administration. The results are shown as the mean ± SD (n = 3) N. S., no significance versus solvent. (D) NB4 cells were incubated with 50 μM CHX and 50 μM GRh2 for 0, 4, 8, and 12 h. Western blot was used to detect PML-RARA expression in NB4 cells after drug administration. A representative picture of three replicates is shown. (E) Quantitative statistical graph of the relative protein expression levels. The results are shown as the mean ± SD (n = 3) $^{*}p < 0.05$. (F) NB4 cells were incubated with 50 μM GRh2 for 8 h. Immunofluorescence was used to detect the formation of PML nuclear bodies (red). Cell nuclei were stained with DAPI (blue) Scale bar=50 μm. (G) NB4 cells were incubated with 30 μM, 40 μM, or 50 μM GRh2 for 12 h. RT-PCR was used to detect the mRNA expression level of *TP53* in NB4 cells after GRh2 administration. The results are shown as the mean ± SD (n = 3) $^{***}p < 0.001$ versus solvent.
GRh2, 20(*S*)-ginsenoside Rh2; PML-RARA, promyelocytic leukemia-retinoic acid receptor A.

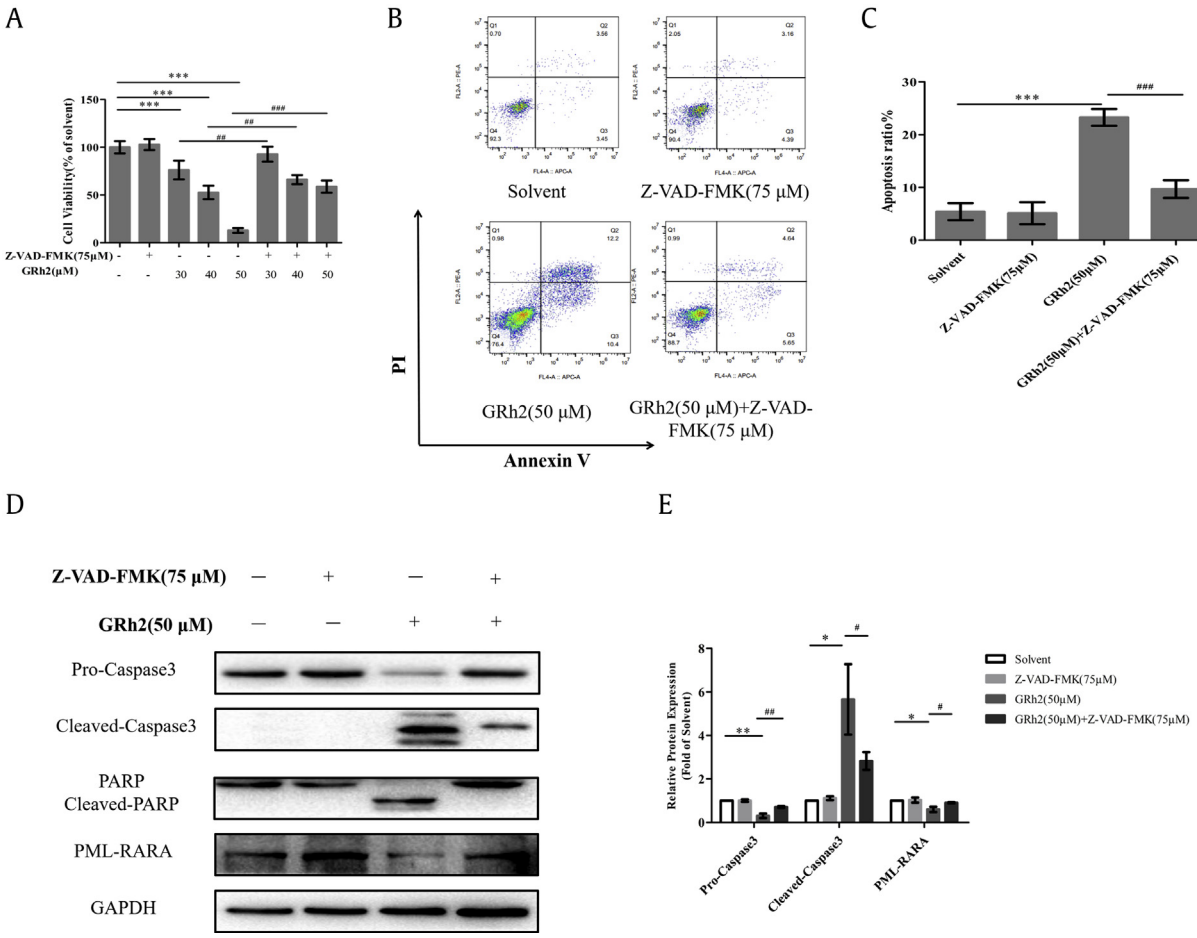

Fig. 5. Apoptosis and PML-RARA degradation in NB4 cells induced by GRh2 were dependent on caspase. After preincubation with 75 μM of Z-VAD-FMK, caspase inhibitor, for 1 h, 30 μM, 40 μM, or 50 μM GRh2 was applied for another 12 h. (A) GRh2 was used with or without Z-VAD-FMK, and the CCK-8 assay measured the NB4 cell viability. The results are shown as the mean ± SD (n = 6) ***$p < 0.001$, ##$p < 0.01$, ###$p < 0.001$. (B) GRh2 (50 μM) was used with or without Z-VAD-FMK. A representative image of the change in the proportion of apoptosis in NB4 cells after drug application, Annexin V/PI double-staining assay was used. (C) Quantitative statistical graph of changes in apoptotic proportions. The results are shown as the mean ± SD (n = 3) ***$p < 0.001$, ###$p < 0.001$. (D) GRh2(50 μM) was applied with or without Z-VAD-FMK. The expression levels of pro-caspase3, cleaved-caspase3, cleaved-PARP, and PML-RARA in NB4 cells were detected via Western blot. A representative picture of three replicates is shown. (E) Quantitative statistical graph of the relative protein expression levels. The results are shown as the mean ± SD (n = 3) *$p < 0.05$, **$p < 0.01$, #$p < 0.05$, ##$p < 0.01$.
GRh2, 20(*S*)-*ginsenoside Rh2; PI, propidium iodide; PML-RARA, promyelocytic leukemia–retinoic acid receptor A.*

cells (Fig. 5D and E). In conclusion, GRh2-induced apoptosis and PML-RARA degradation in NB4 cells depend on caspase.

3.6. GRh2 inhibited the Akt/Bax/caspase9 cascade

The PI3K/Akt signaling pathway is essential in regulating apoptosis and cell survival and is widely activated in leukemia. GRh2 inhibits the Akt signaling pathway and induces apoptosis in cancer cells [20,22–25]. Bax/Bcl-2 and caspase9 are important downstream targets for Akt control of apoptosis [27,32]. Therefore, we further explored whether GRh2 induced upregulation of Bax/Bcl-2 and activation of caspase9 after inhibiting upstream Akt phosphorylation (Fig. 6A and B). The PI3K inhibitor, LY294002, enhanced the antitumor effect of GRh2 (Fig. 6C). Further, after LY294002 was administered alone in NB4 cells, the Bax/Bcl-2 ratio was significantly upregulated (Fig. 6D and E), and caspase3 (Fig. 6D and E) and caspase9 (Fig. 6F) were activated. We suggest that GRh2-induced Bax/Bcl-2 upregulation and caspase9 activation are accompanied by upstream PI3K/Akt pathway inhibition in NB4 cells.

3.7. GRh2 activated the TNF-α/caspase8 cascade

Previous experiments have confirmed that GRh2 induces caspase8 activation in NB4 cells (Fig. 3F). FasL/Fas, TNF-α/TNFR1, and TRAIL/DR4 are caspase8 upstream proteins [18,20]. Many reports describe caspase8 activation induced by FasL/Fas and TNF-α/TNFR1, which are involved in GRh2-induced tumor apoptosis [18,26]. Therefore, we explored whether GRh2-induced caspase8 activation in NB4 cells was achieved by upstream FasL/Fas and TNF-α/TNFR1 activation. Western blot results showed that GRh2 did not significantly affect FasL or Fas expression in NB4 cells, whereas expression of TNF-α and its receptor, TNFR1, were significantly upregulated (Fig. 7A and B). *TNF-α* mRNA levels were also increased (Fig. 7C). C 87, a TNF-α inhibitor, reversed NB4 cell viability, GRh2-mediated apoptosis (Fig. 7D and E), and caspase8 activation (Fig. 7F). Therefore, we believe that GRh2 activates the TNF-α/caspase8 cascade.

4. Discussion

APL is a common acute myeloid leukemia, and the production of the PML-RARA fusion protein is its main driving factor [1–3]. ATO and ATRA can be used to cure APL [2,5], but the adverse reactions

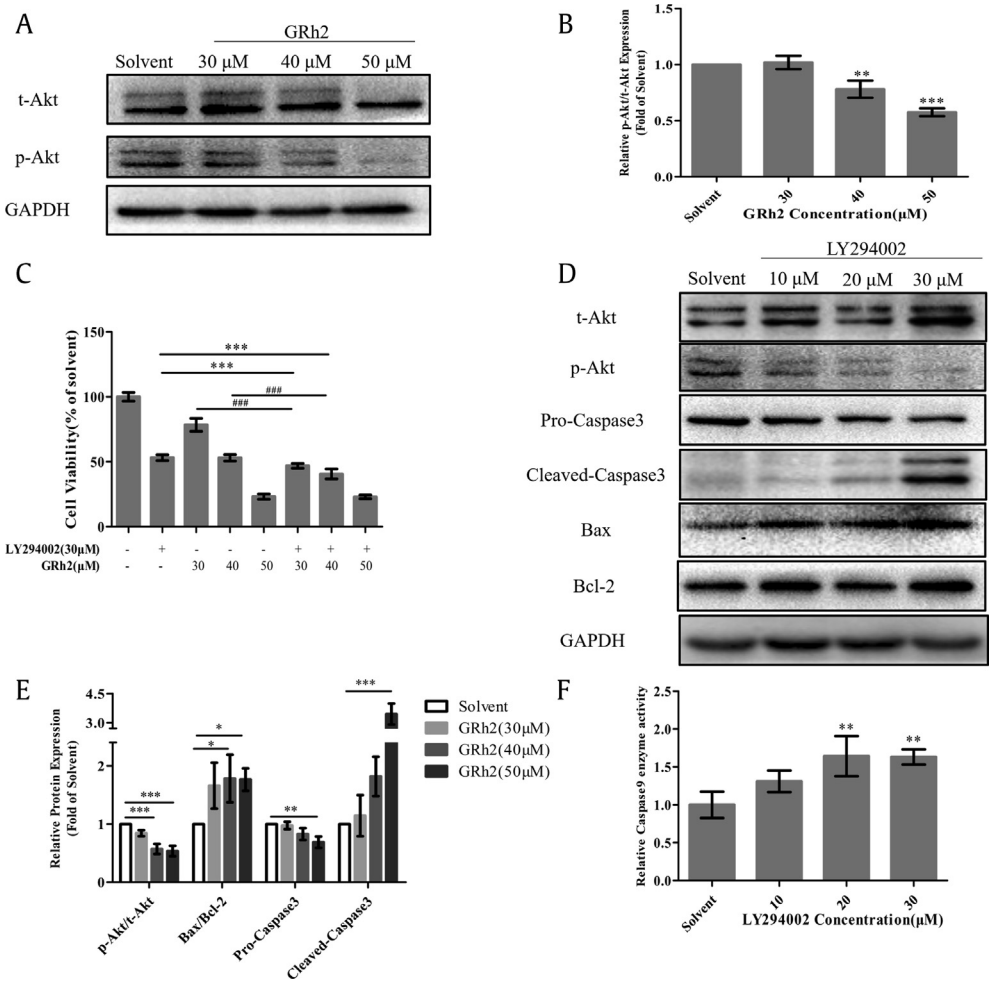

Fig. 6. GRh2 inhibited the Akt/Bax/caspase9 cascade. (A) NB4 cells were incubated with 30 μM, 40 μM, or 50 μM GRh2 for 12 h. The protein expression levels of p-Akt and t-Akt in NB4 cells were detected via Western blot. A representative picture of three replicates is shown. (B) Quantitative statistical graph of the relative protein expression levels. The results are shown as the mean ± SD (n = 3) $^{**}p < 0.01$, $^{***}p < 0.001$ versus solvent. (C) After preincubation with 30 μM PI3K inhibitor LY294002 for 1 h, 30 μM, 40 μM, or 50 μM GRh2 was applied for another 12 h. CCK-8 assay measured the NB4 cell viability. The results are shown as the mean ± SD (n = 6) $^{***}p < 0.001$, $^{###}p < 0.001$. (D) NB4 cells were incubated with 10 μM, 20 μM, or 30 μM LY294002 for 12 h. The expression levels of p-Akt, t-Akt, pro-caspase3, cleaved-caspase3, Bax, and Bcl-2 in NB4 cells were detected via Western blot. A representative picture of three replicates is shown. (E) Quantitative statistical graph of the relative protein expression levels. The results are shown as the mean ± SD (n = 3) $^{*}p < 0.05$, $^{**}p < 0.01$, $^{***}p < 0.001$. (F) The quantitative statistical graph of caspase9 cleavage activation levels in NB4 cells after administering of 10 μM, 20 μM, or 30 μM LY294002 for 12 h. The Ac-LEHD-pNA method was used. The results are shown as the mean ± SD (n = 3) $^{**}p < 0.01$ versus solvent.
GRh2, 20(*S*)-*ginsenoside Rh2.*

severely affect patients' life quality [11]. Therefore, a highly efficient and minimally toxic novel treatment is needed. GRh2 is a major natural anticancer substance extracted from ginseng that is effective against many cancers [14–17]. This study investigated the anti-APL effect of GRh2 *in vitro* and further explored the molecular mechanism of GRh2 against APL. We found that caspase-dependent apoptosis and PML-RARA degradation were regulated via the Akt and TNF-α pathways. Our results suggest that GRh2 is a potential novel treatment for the APL.

Previous studies have shown that GRh2 shows anticancer effects by inducing cell cycle arrest, apoptosis, and autophagy [17–20,23]. Our results verified that GRh2 is one of the most effective anticancer substances in rare diol-type ginsenosides. Compared with other ginsenosides with anticancer effects, GRh2 showed more significant inhibitory effects on viability of the acute promyelocytic leukemia cell line, NB4. Apoptosis and cell cycle arrest were generated, indicating GRh2's antitumor effect against APL *in vitro*.

Mitochondrial oxidation produces substances, such as, ROS, in which free radicals derived from oxygen and their products (ROS) directly or indirectly destroy biological structures, thereby causing irreversible mitochondrial damage and apoptosis [33]. Here, we observed that GRh2 induced ROS production in NB4 cells, which was accompanied by a decreased mitochondrial membrane potential, an increased Bax/Bcl-2 ratio, and activation of caspase family proteins such as caspase8, caspase9, and caspase3. However, NAC application demonstrated that ROS could not mediate the GRh2-induced NB4 cellular mitochondrial damage and apoptosis. Our results indicate that GRh2 induces mitochondrial damage and caspase activation in NB4 cells. ROS is not a signal molecule but an indicator. Other pathways may be involved in GRh2-induced mitochondrial damage.

PML exists in the NBs and plays a role in tumor suppression mainly by activating the *TP53* gene. The PML-RARA fusion protein in NB4 cells destroys PML and the PML NB structure, thus inhibiting the downstream p53 tumor suppressor signaling pathway and leading to unrestricted APL cell proliferation [1–3]. Therefore, degradation of the fusion protein is a key target for inhibiting unrestricted NB4 cell proliferation. Surprisingly, GRh2 induced degradation of PML-RARA fusion proteins, PML NB formation, and activation of the downstream p53 pathway.

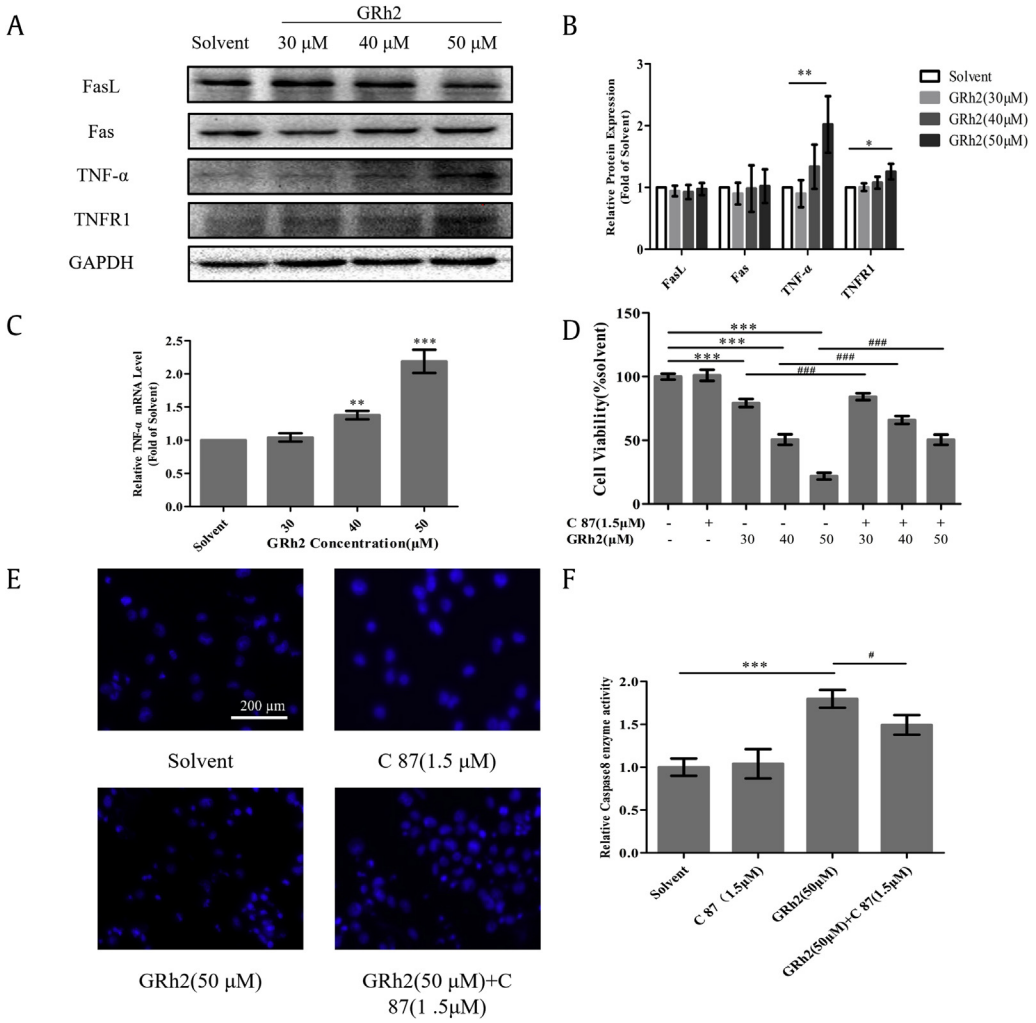

Fig. 7. GRh2 activated the TNF-α/caspase8 cascade. (A) NB4 cells were incubated with 30 μM, 40 μM, or 50 μM GRh2 for 12 h. Protein expression levels of FasL, Fas, TNF-α, and TNFR1 in NB4 cells were detected via Western blot. A representative picture of three replicates is shown. (B) Quantitative statistical graph of the relative protein expression levels. The results are shown as the mean ± SD (n = 3) $^{*}p < 0.05$, $^{**}p < 0.01$. (C) RT-PCR was used to detect the mRNA expression level of *TNF-α* in NB4 cells after GRh2 administration. The results are shown as the mean ± SD (n = 3) $^{**}p < 0.01$, $^{***}p < 0.001$ versus solvent. After preincubation with 1.5 μM TNF-α inhibitor, C 87, for 2 h, 30 μM, 40 μM, or 50 μM GRh2 was applied for another 12 h. (D) CCK-8 assay measured the NB4 cell viability. The results are shown as the mean ± SD (n = 6) $^{***}p < 0.001$, $^{\#\#\#}p < 0.001$. (E) Hoechst 33258 staining was used to observe changes in nuclear morphology of NB4 cells after GRh2 and C 87 administration Scale bar=200 μm. (F) Quantitative statistical graph of caspase8 cleavage activation levels in NB4 cells. The Ac-IETD-pNA method was used. The results are shown as the mean ± SD (n = 3) $^{***}p < 0.001$, $^{\#}p < 0.05$.
GRh2, 20(*S*)-*ginsenoside Rh2.*

PML-RARA degradation mainly depends on proteasomes [3,6], autophagy [7], and caspase [8,9]. From the three mechanisms of PML-RARA degradation described above, as well as caspase, a key target of GRh2, we suspected that GRh2-induced fusion protein degradation was dependent on caspase cleavage activation. Therefore, we applied Z-VAD-FMK, a broad-spectrum caspase inhibitor, which reversed the GRh2-induced apoptosis of NB4 cells. Surprisingly, Z-VAD-FMK reversed the GRh2-induced PML-RARA degradation in NB4 cells. These findings suggest that GRh2 induced caspase-dependent apoptosis and PML-RARA fusion protein degradation in NB4 cells .

Two pathways are involved in apoptosis: the death receptor pathway and the mitochondrial pathway. The former is mainly mediated by Bax/Bcl-2, cytochrome c, and caspase9 [34,35], and the latter is mainly mediated by caspase8, which together activate caspase3, a key effector molecule in apoptosis, thus causing irreversible DNA fragmentation cleavage [36]. The PI3K/Akt signaling cascade is abnormally activated in a variety of cancer cells, which can inhibit cell apoptosis and promote cell survival [22,23]. Inhibition of the PI3K/Akt signaling pathway can activate the Bax/caspase9 signaling cascade and initiate the mitochondrial apoptosis pathway [27,32]. Our study found that GRh2 significantly reduced the proportion of p-Akt/t-Akt in NB4 cells. Additionally, the PI3K inhibitor, LY294002, showed synergistic antitumor effects with GRh2. LY294002 alone induced increased Bax and cleaved caspase3 protein levels and caspase9 activation, further indicating that PI3K/Akt pathway inhibition is closely related to Bax/caspase9 activation in NB4 cells. This confirmed that induction of the Bax/caspase9 cascade by GRh2 depended on the PI3K/Akt pathway blockade. The major upstream regulators of the death receptor pathway include four classes: TNF-α/TNFR, Fas/FasL, TRAIL, and DR4 [18,20,36]. TNF-α/TNFR and Fas/FasL are the most critical signaling pathways for GRh2-induced apoptosis [18,26]. Therefore, we explored the upstream molecules of caspase8 in these two pathways. We observed no changes in the expressions of FasL or its receptor Fas during GRh2-induced apoptosis in NB4 cells. However, we observed a significant upregulation of TNF-α. Applying the TNF-α inhibitor, C 87, significantly reversed NB4 cell viability, GRh2-mediated

apoptosis, and caspase8 activation. Our results suggest that the TNF-α signaling pathway is involved in GRh2 activating caspase8.

In conclusion, this study revealed that GRh2 significantly induced a decrease in NB4 cell viability, mainly manifested via cell cycle arrest and apoptosis. GRh2-induced apoptosis of NB4 cells was accompanied by mitochondrial damage and cleavage activation of caspase3, caspase8, and caspase9. GRh2 also induced PML-RARA degradation and initiated the p53 tumor suppressor signaling pathway in NB4 cells, which was caspase-dependent and regulated by upstream Akt/Bax/caspase9 and TNF-α/caspase8 signaling pathways. These results suggest that GRh2 is a potential candidate for APL treatment. Its high efficiency and low toxicity give it broad application prospects.

Declaration of competing interest

All authors declare no conflict of interest.

Acknowledgments

The authors thank the Jiangsu Key Laboratory for Pharmacology and Safety Evaluation of Chinese Materia Medica for technical and equipment support for this study.

Appendix A. Supplementary data

Supplementary data to this article can be found online at https://doi.org/10.1016/j.jgr.2020.05.001.

References

[1] Chen S, Fang Y, Ma L, Liu S, Li X. Realgar-induced apoptosis and differentiation in all-trans retinoic acid (ATRA)-sensitive NB4 and ATRA-resistant MR2 cells. Int J Oncol 2012;40:1089–96.
[2] Nasr R, Lallemand-Breitenbach V, Zhu J, Guillemin MC, de The H. Therapy-induced PML/RARA proteolysis and acute promyelocytic leukemia cure. Clin Cancer Res 2009;15:6321–6.
[3] Li K, Wang F, Cao WB, Lv XX, Hua F, Cui B, Yu JJ, Zhang XW, Shang S, Liu SS, et al. TRIB3 promotes APL progression through stabilization of the oncoprotein PML-RARalpha and inhibition of p53-mediated senescence. Cancer Cell 2017;31:697–710.
[4] Watts JM, Tallman MS. Acute promyelocytic leukemia: what is the new standard of care? Blood Rev 2014;28:205–12.
[5] Chen SJ, Zhou GB, Zhang XW, Mao JH, de The H, Chen Z. From an old remedy to a magic bullet: molecular mechanisms underlying the therapeutic effects of arsenic in fighting leukemia. Blood 2011;117:6425–37.
[6] Yoshida H, Kitamura K, Tanaka K, Omura S, Miyazaki T, Hachiya T, Ohno R, Naoe T. Accelerated degradation of PML-retinoic acid receptor alpha (PML-RARA) oncoprotein by all-trans-retinoic acid in acute promyelocytic leukemia: possible role of the proteasome pathway. Cancer Res 1996;56:2945–8.
[7] Isakson P, Bjoras M, Boe SO, Simonsen A. Autophagy contributes to therapy-induced degradation of the PML/RARA oncoprotein. Blood 2010;116:2324–31.
[8] Wang X, Lin Q, Lv F, Liu N, Xu Y, Liu M, Chen Y, Yi Z. LG-362B targets PML-RAR alpha and blocks ATRA resistance of acute promyelocytic leukemia. Leukemia 2016;30:1465–74.
[9] Tong Q, You H, Chen X, Wang K, Sun W, Pei Y, Zhao X, Yuan M, Zhu H, Luo Z, et al. ZYH005, a novel DNA intercalator, overcomes all-trans retinoic acid resistance in acute promyelocytic leukemia. Nucleic Acids Res 2018;46:3284–97.
[10] Nervi Clara, Ferrara Fabiana F, Fanelli Mirco, Rippo Maria Rita, Tomassini Barbara, Ferrucci Pier Francesco, Ruthardt Martin, Gelmetti Vania, Gambacorti-Passerini Carlo, Diverio Daniela, et al. Caspases mediate retinoic acid-induced degradation of the acute promyelocytic leukemia PML/RARa fusion protein. Blood 1998;92:2244–51.
[11] Lo-Coco F, Avvisati G, Vignetti M, Thiede C, Orlando SM, Iacobelli S, Ferrara F, Fazi P, Cicconi L, Di Bona E, et al. Retinoic acid and arsenic trioxide for acute promyelocytic leukemia. N Engl J Med 2013;369:111–21.
[12] Burnett AK, Russell NH, Hills RK, Bowen D, Kell J, Knapper S, Morgan YG, Lok J, Grech A, Jones G, et al. Arsenic trioxide and all-trans retinoic acid treatment for acute promyelocytic leukaemia in all risk groups (AML17): results of a randomised, controlled, phase 3 trial. Lancet Oncology 2015;16:1295–305.
[13] Kamimura T, Miyamoto T, Harada M, Akashi K. Advances in therapies for acute promyelocytic leukemia. Cancer Sci 2011;102:1929–37.
[14] Qian J, Li J, Jia JG, Jin X, Yu DJ, Guo CX, Xie B, Qian LY. Ginsenoside-Rh2 inhibits proliferation and induces apoptosis of human gastric cancer SGC-7901 side population cells. Asian Pac J Cancer Prev 2016;17:1817–21.
[15] Chen F, Deng Z, Xiong Z, Zhang B, Yang J, Hu J. A ROS-mediated lysosomal-mitochondrial pathway is induced by ginsenoside Rh2 in hepatoma HepG2 cells. Food Funct 2015;6:3828–37.
[16] Lee H, Lee S, Jeong D, Kim SJ. Ginsenoside Rh2 epigenetically regulates cell-mediated immune pathway to inhibit proliferation of MCF-7 breast cancer cells. J Ginseng Res 2018;42:455–62.
[17] Chung KS, Cho SH, Shin JS, Kim DH, Choi JH, Choi SY, Rhee YK, Hong HD, Lee KT. Ginsenoside Rh2 induces cell cycle arrest and differentiation in human leukemia cells by upregulating TGF-beta expression. Carcinogenesis 2013;34:331–40.
[18] Guo XX, Li Y, Sun C, Jiang D, Lin YJ, Jin FX, Lee SK, Jin YH. p53-dependent Fas expression is critical for Ginsenoside Rh2 triggered caspase-8 activation in HeLa cells. Protein Cell 2014;5:224–34.
[19] Wang C, He H, Dou G, Li J, Zhang X, Jiang M, Li P, Huang X, Chen H, Li L, et al. Ginsenoside 20(S)-Rh2 induces apoptosis and differentiation of acute myeloid leukemia cells: role of orphan nuclear receptor Nur77. J Agric Food Chem 2017;65:7687–97.
[20] Chen F, Zheng SL, Hu JN, Sun Y, He YM, Peng H, Zhang B, McClements DJ, Deng ZY. Octyl ester of ginsenoside Rh2 induces apoptosis and G1 cell cycle arrest in human HepG2 cells by activating the extrinsic apoptotic pathway and modulating the akt/p38 MAPK signaling pathway. J Agric Food Chem 2016;64:7520–9.
[21] Guo XX, Guo Q, Li Y, Lee SK, Wei XN, Jin YH. Ginsenoside Rh2 induces human hepatoma cell apoptosisvia bax/bak triggered cytochrome c release and caspase-9/caspase-8 activation. Int J Mol Sci 2012;13:15523–35.
[22] Aoki M, Fujishita T. Oncogenic roles of the PI3K/AKT/mTOR Axis. Curr Top Microbiol Immunol 2017;407:153–89.
[23] Xia T, Zhang J, Zhou C, Li Y, Duan W, Zhang B, Wang M, Fang J. 20(S)-Ginsenoside Rh2 displays efficacy against T-cell acute lymphoblastic leukemia through the PI3K/Akt/mTOR signal pathway. Journal of Ginseng Research 2019.
[24] Steelman LS, Abrams SL, Whelan J, Bertrand FE, Ludwig DE, Basecke J, Libra M, Stivala F, Milella M, Tafuri A, et al. Contributions of the Raf/MEK/ERK, PI3K/PTEN/Akt/mTOR and Jak/STAT pathways to leukemia. Leukemia 2008;22:686–707.
[25] Li KF, Kang CM, Yin XF, Li HX, Chen ZY, Li Y, Zhang Q, Qiu YR. Ginsenoside Rh2 inhibits human A172 glioma cell proliferation and induces cell cycle arrest status via modulating Akt signaling pathway. Mol Med Rep 2018;17:3062–8.
[26] Huang J, Peng K, Wang L, Wen B, Zhou L, Luo T, Su M, Li J, Luo Z. Ginsenoside Rh2 inhibits proliferation and induces apoptosis in human leukemia cells via TNF-alpha signaling pathway. Acta Biochim Biophys Sin (Shanghai) 2016;48:750–5.
[27] Yuan J, Deng Y, Zhang Y, Gan X, Gao S, Hu H, Hu S, Hu J, Liu H, Li L, et al. Bmp4 inhibits goose granulosa cell apoptosis via PI3K/AKT/caspase-9 signaling pathway. Anim Reprod Sci 2019;200:86–95.
[28] Gabert J, Beillard E, van der Velden VHJ, Bi W, Grimwade D, Pallisgaard N, Barbany G, Cazzaniga G, Cayuela JM, Cave H, et al. Standardization and quality control studies of 'real-time' quantitative reverse transcriptase polymerase chain reaction of fusion gene transcripts for residual disease detection in leukemia-A Europe against Cancer Program. Leukemia 2003;17:2318–57.
[29] Sun M, Ye Y, Xiao L, Duan XY, Zhang YM. Anticancer effects of ginsenoside Rg3 (review). Int J Mol Med 2017;39:507–18.
[30] Zhang X, Zhang SL, Sun QT, Jiao WJ, Yan Y, Zhang XW. Compound K induces endoplasmic reticulum stress and apoptosis in human liver cancer cells by regulating STAT3. Molecules 2018;23:1482.
[31] Gianni M. In acute promyelocytic leukemia NB4 cells, the synthetic retinoid CD437 induces contemporaneously apoptosis, a caspase-3-mediated degradation of PML/RARα protein and the PML retargeting on PML-nuclear bodies. Leukemia 1999;13:739–49.
[32] Simonyan L, Renault TT, Novais MJ, Sousa MJ, Corte-Real M, Camougrand N, Gonzalez C, Manon S. Regulation of Bax/mitochondria interaction by AKT. FEBS Lett 2016;590:13–21.
[33] Sun S, Zhang C, Gao J, Qin Q, Zhang Y, Zhu H, Yang X, Yang D, Yan H. Benzoquinone induces ROS-dependent mitochondria-mediated apoptosis in HL-60 cells. Toxicol Ind Health 2018;34:270–81.
[34] Green DR, Kroemer G. The pathophysiology of mitochondrial cell death. Science 2004;305:626–9.
[35] Shimizu S, Narita M, Tsujimoto Y. Bcl-2 family proteins regulate the release of apoptogenic cytochrome c by the mitochondrial channel VDAC. Nature 1999;399:483–7.
[36] Ashkenazi A, Dixit VM. Death receptors: signaling and modulation. Science 1998;281:1305–8.